23rd International Congress on Sound & Vibration
Athens, Greece 10-14 July 2016
ICSV23

RESPONSE OF SWIRL-STABILIZED PERFECTLY PREMIXED FLAME TO HIGH-AMPLITUDE VELOCITY EXCITATIONS

Dmytro Iurashev
Università degli studi di Genova, via Montallegro, 1 - 16145, Genoa, Italy
email: dmytro.iurashev@edu.unige.it

Giovanni Campa and Vyacheslav V. Anisimov
Ansaldo Energia S.p.A., via Nicola Lorenzi, 8 - 16152, Genoa, Italy

Currently, gas turbines manufacturers frequently face the problem of strong acoustic combustion driven oscillations inside combustion chambers. These combustion instabilities can cause extensive wear and sometimes even catastrophic damage of combustion hardware. Some types of analysis predicts only unsteady frequencies of combustion systems based on the knowledge of the flame response to velocity perturbations of small amplitude. However, gas turbines manufacturers are interested not only in the unsteady frequencies of acoustic oscillations, but in the amplitude of such oscillations as well, in order to determine how these oscillations are harmful for their equipment. To calculate these oscillations amplitudes it is not enough to know how the flame responses to the small-amplitude acoustic perturbations but it is also necessary to know how the flame responds to acoustic perturbations of high amplitude. In this work we consider a swirl-stabilized perfectly premixed test rig developed at the Technische Universität München. We perform a set of Unsteady Reynolds-Averaged Navier-Stokes (URANS) simulations with the Flame Speed Closure (FSC) model implemented in OpenFOAM environment to obtain the Flame Describing Function (FDF) of the combustor setup. We extend an already existing linear physically meaningful model for the flame in this setup to the non-linear regime. We analyse the cause factors for changes in the model parameters when applying high-amplitude velocity perturbations.

1. Introduction

Nowadays gas turbine manufacturers have to meet ecological requirements, particularly emissions of NO_X. These requirements force to produce gas turbines that work in lean combustion regime. However, the operation in lean combustion regime is characterized by high probability of combustion instabilities occurrence [1, 2, 3], which may cause catastrophic damages.This requires prevention of combustion instabilities, which, in turn, requires understanding of the nature of their occurrence.

Often researchers and engineers perform linear stability analyses. This type of analysis allows to predict stable and unstable frequencies of thermoacoustic systems and makes use of the Flame Transfer Function (FTF) - the response of the flame to small amplitude velocity perturbations [4]. To forecast not only the frequency of pressure oscillations, but also their amplitude, the Flame Describing Function (FDF) - the response of the flame to velocity perturbations at different amplitudes - should be known both for analyses in the frequency domain [5] and for analyses in the time domain [6]. To predict the occurrence of combustion instabilities at the design stage it is necessary to understand the connections between acoustics and combustion.

In this work we investigate combustion dynamics with the help of Unsteady Reynolds-Averaged Navier-Stokes (URANS) simulations using Flame Speed Closure (FSC) model [7] implemented in OpenFOAM environment [8]. In particular, we discuss the Beschaufelter RingSpalt (BRS) test rig developed by Komarek and Polifke [9] at the Technische Universität München. In ref. [9] the authors investigate the response of the flame to axial and tangential components of velocity excitations for a perfectly premixed swirl-stabilized flames and propose an analytical model for the flame response to velocity excitations. However, this model covers only the linear regime of excitations. In this paper we extend the analysis of ref. [9] performing simulations with different amplitudes of velocity excitations at several frequencies, obtaining the Flame Describing Function (FDF). The obtained FDF is then approximated with an analytical model.

2. Background

2.1 Description of the Flame Speed Closure model

In order to model the combustion in the BRS test rig we use Flame Speed Closure (FSC) model proposed by Lipatnikov and Chomiak [7]. This flame model was implemented into the *XiFoam* solver of OpenFOAM [10]. This is a solver for simulation of compressible premixed/partially-premixed combustion with turbulence modeling. It uses compressible PIMPLE (merged PISO-SIMPLE) algorithm and solves the transport equation for the regress variable b.

The FSC model describes the propagation of the flame in the limit case of the absence of turbulence as well as in the case of fully developed turbulence. Moreover, it takes into account the dependence of turbulent diffusivity and turbulent flame speed on the time of flow propagation from the flame holder to the flame front. Further details on the FSC model can be found in [7] and [8].

2.2 Flame Transfer Function

The dynamic response of a flame to a flow perturbation of small amplitudes can be represented in the frequency domain by its Flame Transfer Function $FTF(\omega)$ (also called "frequency response of the flame"). It relates fluctuations of the flame heat release $\dot{Q}'$ to fluctuations of mass flow rate or velocity u'_r at a reference position r upstream of the flame normalized by the mean values of heat release $\bar{\dot{Q}}$ and velocity $\bar{u}_r$ respectively

$$FTF(\omega) = \frac{\dot{Q}'(\omega)/\bar{\dot{Q}}}{u'_r(\omega)/\bar{u}_r}. \tag{1}$$

Application of the Wiener-Hopf inversion (WHI) to results of unsteady CFD simulations in order to find the FTF of a burner was initially proposed by Polifke et al. [11]. This method reconstructs the Unit Impulse Response (UIR) of the flame to the velocity perturbation and then transforms it into the frequency response using the z-transform:

$$FTF(\omega) = \sum_{k=0}^{L} h_k e^{-i\omega k\Delta t}, \tag{2}$$

where h_k are coefficients of the UIR; to find them, the auto-correlation matrix Γ and the cross-correlation vector $\mathbf{c}$ of the time series data $(u'_k, \dot{Q}'_k)$ for $k = 0, ..., N$ are calculated as follows:

$$\Gamma_{ij} = \frac{1}{N-L+1}\sum_{k=L}^{N} \frac{u'_{k-i}}{\bar{u}}\frac{u'_{k-j}}{\bar{u}} \text{ for } i,j = 0, ..., L, \tag{3}$$

$$c_i = \frac{1}{N-L+1}\sum_{k=L}^{N} \frac{u'_{k-i}}{\bar{u}}\frac{\dot{Q}'_k}{\bar{\dot{Q}}} \text{ for } i = 0, ..., L, \tag{4}$$

where N is the number of points in vector of the signal time series, L is assumed length of the vector of the UIR, the filter "memory". To find the vector of coefficients of the UIR, the WHI is performed

$$\mathbf{h} = \Gamma^{-1}\mathbf{c}. \tag{5}$$

2.3 Flame Describing Function

In general, the response of the flame to velocity perturbations depends not only on the frequency of the perturbation but also on its amplitude. Thus, if one would like to perform amplitude-dependent stability analysis of a thermo-acoustic system, the Flame Describing Function (FDF), should be known:

$$FDF(\omega, A) = \frac{\dot{Q}'(\omega, A)/\bar{\dot{Q}}}{u_r'(\omega, A)/\bar{u}_r} \tag{6}$$

where A is the normalized amplitude of velocity perturbations at the reference point.

Unfortunately, advanced methods, such as WHI can be used only in linear cases, i.e. response of the flame to small amplitudes of velocity perturbations. Thus, in order to compute the FDF we have to apply only one frequency excitation with one amplitude per simulation.

3. Modeling the Flame Describing Function

3.1 Description of the experimental setup

The test rig under consideration is a swirl stabilized atmospheric burner with a central bluff body (see Fig. 1). Methane is burnt in the lean combustion region. Perfectly premixed mixture of methane and the air with equivalence ratio equal to 0.77 enters in the setup. The burner exit is represented by an annular section with an inner diameter of $16\ mm$ and an outer diameter of $40\ mm$. The swirler consists of 8 blades with length of $30\ mm$ and is positioned $30\ mm$ upstream the burner exit. Combustion chamber has a quadratic cross-section of $90 \times 90\ mm^2$. The length of the combustion chamber is variable and during FTF measurements was kept equal to $300\ mm$. Further details about experimental set-up can be found in ref. [9].

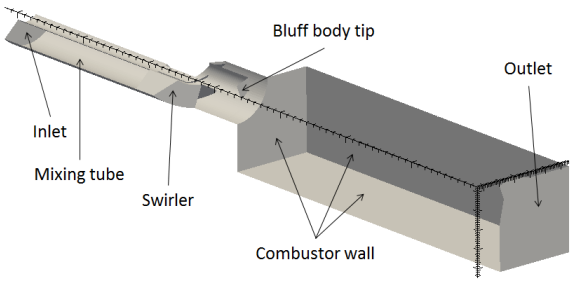

Figure 1: Sector scheme of the numerical set-up of the BRS test rig

A 3D structured mesh consisting of around 280000 cells is created using the commercial software ANSYS ICEM CFD. Since the structure of the set-up is periodical, just one quarter of the test rig is modeled in the simulations. Instead of the actual $300\ mm$ combustor length that was used in the experiments, in the numerical simulation the combustor length is fixed at $200\ mm$ to lower the computational effort. The different length does not influence the computed FDF because the heat release zone lays in the first $100\ mm$ of the combustion chamber, as reported in [9]. The time step of the simulations is $4 \times 10^{-7} s$ to ensure an acoustic CFL number lower than 0.7.

In investigation the thermal power equal to $30\ kW$. To avoid the development of resonant modes, non-reflective or partially reflective boundary conditions at the inlet and at the outlet have been employed. We make use of the *waveTransmissive* boundary condition that is implemented in OpenFOAM [10] and is based on the work of Poinsot and Lele [12].Boundary conditions for the unperturbed simulation are listed in Table 1. In a previous work of ours [8] a sensitivity analysis of the parameters of the FSC model was done. As a result, the following values of parameters were chosen: $Sc_t = 0.3$, $C_D = 0.3$ and $u_{FSC} = 18\ m/s$. The results of unperturbed simulations could be found in [8].

Table 1: Boundary Conditions for the BRS numerical model

Face	**Boundary condition**	**Details**
Inlet	Velocity inlet	$11.3\ m/s$
Outlet	Pressure outlet	$101325\ Pa$
Mixing tube, swirler	Adiabatic no-slip wall	–
Combustor wall	Isothermal no-slip wall	$600\ K$
Bluff body tip	Isothermal no-slip wall	$600\ K$

3.2 Numerically obtained FTF

A transient numerical simulation of the system is performed exciting the velocity at the inlet of the computational domain. The signal of excitation is composed of a sum of sines with random frequency in range $0 - 1\ kHz$ and random phase. The amplitude of the excitation signal is calculated in a way that three standard deviations of the signal are equal to 10% of the mean velocity at the inlet of the computational domain.

The time series u_r is computed during the simulations as the axial velocity component averaged in the plane perpendicular to the longitudinal axis situated 2 cm upstream of the burner exit (1 cm downstream of the swirler). The response of the flame $\dot{Q}$ is measured in the simulations as the volumetric integral in the whole combustor of the source term in the transport equation for the regress variable. The mean values $\bar{u}_r$, $\bar{\dot{Q}}$ and fluctuations u'_r, $\dot{Q}'$ are computed from the measured time series u_r, $\dot{Q}$

The simulation is run for $129\ ms$ in real time. Simulations run with longer times do not yield appreciable change of the FTF. The length of the UIR was assumed to be equal to $10\ ms$. The first $15\ ms$ are considered as transition period and are neglected. Using Wiener-Hopf inversion method described before, the Flame Transfer Function of the BRS test rig is calculated. The resulting FTF is shown in Fig. 2.

3.3 Numerically obtained FDF

In order to construct the Flame Describing Function, excitation frequencies of $100\ Hz$, $160\ Hz$, $240\ Hz$ and $320\ Hz$ are chosen. $100\ Hz$, $240\ Hz$ and $320\ Hz$ are local extrema of the FTF gain shown in Fig. 2. To ensure that the difference of the FDF phase between $100\ Hz$ and $240\ Hz$ is smaller than π, the $160\ Hz$ is also considered. Different excitation amplitudes of velocity perturbations are applied at the inlet of the numerical setup in order to obtain velocity perturbations after the swirler with amplitude of 30%, 50% and 70% for each frequency.

The FDF obtained from the simulations is shown in Fig. 2. The most significant decay of the gain of the FDF with increasing amplitude of the velocity perturbations is observed at $100\ Hz$ (see Fig. 2). The most significant change in phase of the FDF is observed at $240\ Hz$ (see Fig. 2). The decrease of the FDF phase absolute value at this frequency could be explained by the fact that the flame enters inside the mixing tube when forced with high level amplitudes (see Figs. 4, 5).

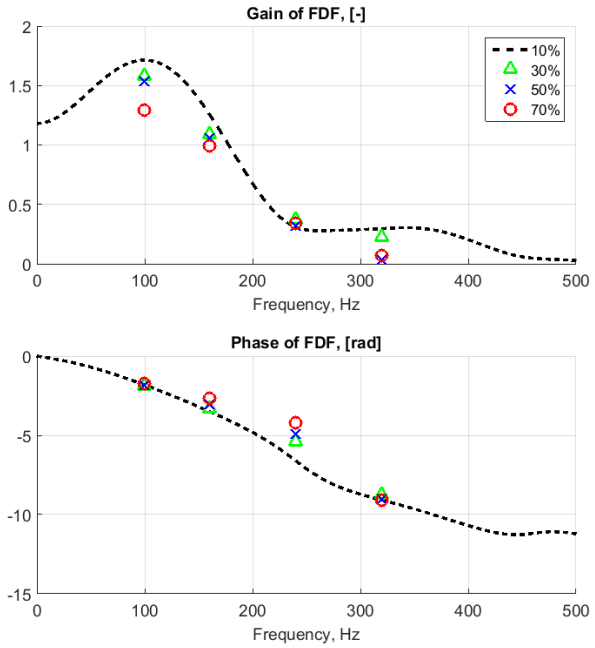

Figure 2: FTF (dashed line) and FDF (points) of the BRS obtained from simulations

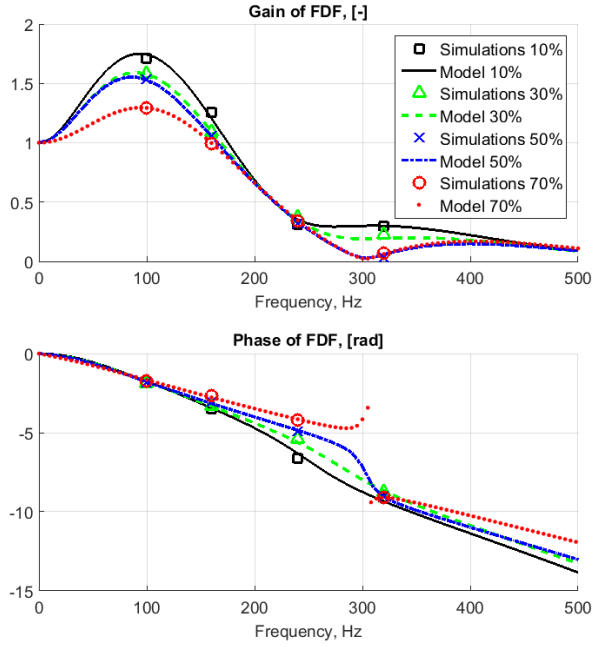

Figure 3: FDF modeled with Eq. 8 and values of τ_i and σ_i from Table 2

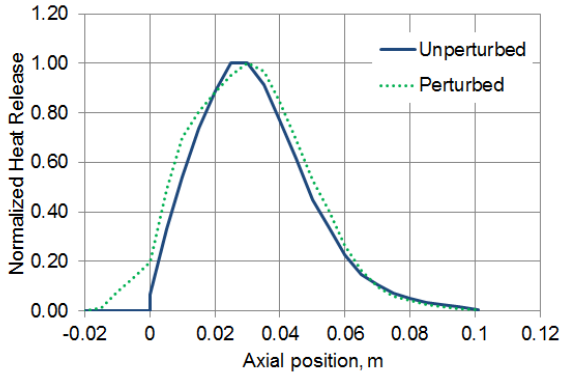

Figure 4: Heat release distribution in the setup without perturbation and heat release distribution averaged over one period of oscillation (excitation at *240 Hz* with the amplitude 70%)

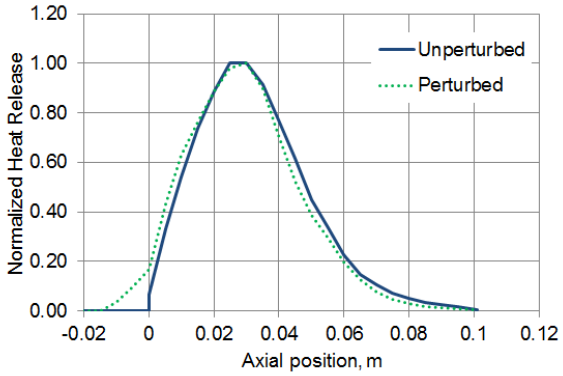

Figure 5: Heat release distribution in the setup without perturbation and heat release distribution averaged over one period of oscillation (excitation at *320 Hz* with the amplitude 70%)

4. Analytical model for the FDF

Komarek and Polifke [9] have proposed the following model for the FTF in the case of perfectly premixed swirl-stabilized combustion

$$FTF(\omega) = e^{-i\omega\tau_1 - 0.5\omega^2\sigma_1^2} + a\left(e^{-i\omega\tau_2 - 0.5\omega^2\sigma_2^2} - e^{-i\omega\tau_3 - 0.5\omega^2\sigma_3^2}\right) \tag{7}$$

where τ_i is the time delay of the corresponding mechanism, σ_i is the standard deviation of the corresponding time delay and a is the dimensionless constant. The response of the flame to the axial perturbations of velocity is modeled with parameters τ_1 and σ_1. τ_2, σ_2, τ_3 and σ_3 model the response of the heat release to the tangential perturbations of velocity produced by a swirler. With respect to the original model [9], Tay-Wo-Chong et al. [13] introduced the dimensionless parameter $a = 1.05$ that gives a better agreement with the measured FTF.

In this paper the model in Eq. (7) is extended to the nonlinear regime introducing the dependence

of the parameters τ_i and σ_i on the amplitude of velocity excitation

$$FDF(\omega, A) = e^{-i\omega\tau_1(A)-0.5[\omega\sigma_1(A)]^2} + a\left(e^{-i\omega\tau_2(A)-0.5[\omega\sigma_2(A)]^2} - e^{-i\omega\tau_3(A)-0.5[\omega\sigma_3(A)]^2}\right) \tag{8}$$

Firstly, we find the optimum values of τ_i and σ_i for each amplitude of velocity perturbations using the method of least squares. The obtained values of parameters τ_i and σ_i for different amplitudes of perturbation are presented in Table 2 and the corresponding modeled FDF is shown in Fig. 3. All τ_i decrease with increasing A. This trend is explained by the flame shifting towards the swirler when forced with high excitation amplitudes. σ_1 decreases while increasing A. On the contrary, σ_2 and σ_3 increase while increasing A.

Table 2: Values of parameters τ_i and σ_i for different amplitudes of perturbation, *ms*

Amplitude	τ_1	σ_1	τ_2	σ_2	τ_3	σ_3
10%	2.43	0.93	4.40	0.73	6.25	1.33
30%	2.47	0.92	4.18	0.73	5.71	1.81
50%	2.33	0.78	3.98	0.77	5.27	2.38
70%	1.95	0.73	3.60	0.77	3.35	2.44

Secondly, the dependence of τ_i and σ_i on the normalized amplitude of velocity perturbations A are modeled as

$$\tau_i = \tau_{i,0} + \tau_{i,2}A^2 \tag{9}$$

$$\sigma_i = \sigma_{i,0} + \sigma_{i,1}A \tag{10}$$

Quadratic dependence of τ_i on A is chosen because it gives smaller values of root-mean-square errors than a linear dependence. For $\sigma_i(A)$ a linear dependence gives the smallest values of root-mean-square errors. Optimal values of parameters $\tau_{i,0}$, $\tau_{i,2}$, $\sigma_{i,0}$ and $\sigma_{i,1}$ are found using the least squares method and are listed in Table 3. The resulting functions are shown in Fig. 6 together with the values from Table 2.

Table 3: Values of parameters $\tau_{i,0}$, $\tau_{i,2}$, $\sigma_{i,0}$ and $\sigma_{i,1}$, *ms*

i	$\tau_{i,0}$	$\tau_{i,2}$	$\sigma_{i,0}$	$\sigma_{i,1}$
1	2.52	-1.07	0.99	-0.37
2	4.38	-1.60	0.72	0.08
3	6.37	-5.85	1.21	1.95

The physical meaning of parameters τ_i and σ_i and of their dependence on A is understood if we switch from the frequency domain representation of the FTF to the time domain representation, i.e. to the Unit Impulse Response (UIR). The UIR in this work is the response of the normalized heat release to the normalized velocity perturbation of unit amplitude. The analytical form of the UIR corresponding to the FTF of Eq. 7 is

$$UIR(t) = \frac{1}{\sigma_1\sqrt{2\pi}}e^{-\frac{1}{2}\left(\frac{t-\tau_1}{\sigma_1}\right)^2} + a\left(\frac{1}{\sigma_2\sqrt{2\pi}}e^{-\frac{1}{2}\left(\frac{t-\tau_2}{\sigma_2}\right)^2} - \frac{1}{\sigma_3\sqrt{2\pi}}e^{-\frac{1}{2}\left(\frac{t-\tau_3}{\sigma_3}\right)^2}\right) \tag{11}$$

The UIR for different amplitudes of velocity excitation are shown in Fig. 7. As it can be observed, higher velocity perturbations amplitudes cause the flame response peaks to occur earlier in

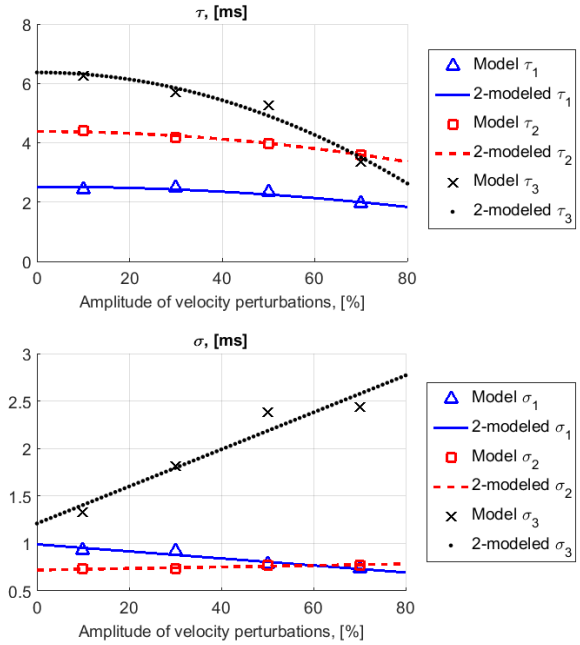

Figure 6: Dependencies $\tau_i(A)$ and $\sigma_i(A)$ from Table 2 (points, "Model") and modeled by Eqs. (9)-(10) (lines, "2-modeled")

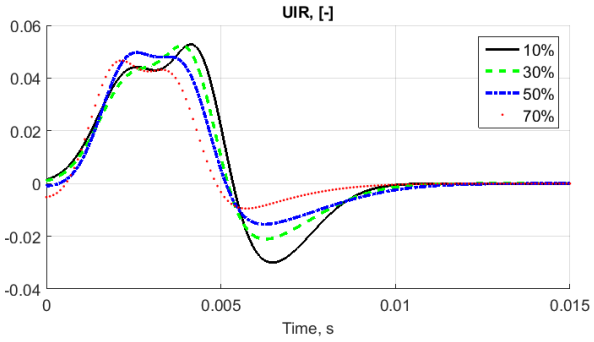

Figure 7: UIRs for different amplitudes of velocity excitations modeled by Eq. (11) with values of parameters τ_i and σ_i from Table 2

time. Furthermore, the overall response duration remains almost the same for the 4 cases considered. The different shapes of the UIR could be explained as follows. When the high-amplitude velocity oscillation experiences its minimum values, locally the turbulent flame velocity is higher than the axial velocity component causing the flame front to be pushed behind the flame-holder and towards the swirler. This shift in the flame position results in a decrease of τ_i with increasing A. On the contrary, when the high amplitude velocity oscillation experiences its maximum values, the flow pushes the flame from the flame holder towards the exit of the combustor. Thus, the length of the heat release averaged over one period of oscillation becomes higher. The prolongation of the flame results in higher dispersion of the heat release averaged over one period and, thus, in a higher dispersion of the UIR. The comparison between the heat release distribution without excitation and the heat release distribution averaged over one period of oscillation shown in Figs. 4 and 5 supports this explanation.

5. Conclusions

In this work we have calculated the Flame Describing Function of the perfectly premixed swirl-stabilized test-rig performing URANS simulations with the Flame Speed Closure model implemented in OpenFOAM. Using obtained FDF we have extended the linear model for the heat release response in the perfectly premixed swirl-stabilized combustion systems to the non-linear regime introducing dependencies of the parameters of the model on the amplitude of velocity excitations. We have found how the response of the flame to velocity oscillations changes while changing the amplitude of velocity perturbations. We have also provided a possible explanation of such changes of the flame response considering averaged distribution of the heat release during one period of oscillations with high amplitude excitations.

Acknowledgements

The presented work is part of the Marie Curie Initial Training Network Thermo-acoustic and aero-acoustic nonlinearities in green combustors with orifice structures (TANGO). We gratefully ac-

knowledge the financial support from the European Commission under call FP7-PEOPLE-ITN-2012. Dmytro Iurashev would like to acknowledge Alp Albayrak for familiarizing himself with the BRS setup and for the consultancy in OpenFOAM environment.

REFERENCES

1. Lieuwen, T. C. and Yang, V. *Acoustic analysis of gas turbine combustors*, American Institute of Aeronautics and Astronautics, (2005).

2. Huang, Y., Yang, V., Dynamics and stability of lean-premixed swirl-stabilized combustion, *Progress in Energy and Combustion Science,* **35**, 293–364, (2009)

3. Sirignano, W.A. Driving mechanisms for combustion instability, *London Edinburgh and Dublin Philosophical Magazine and Journal of Science*, **17**, 419–422, (2015).

4. Rofi, L., Campa, G., Anisimov, V., Daccá, F., Bertolotto, E., Gottardo, E., Bonzani, F., Numerical procedure for the investigation of combustion dynamics in industrial gas turbines: LES, RANS and thermoacoustics, *ASME paper GT2015-42168,* (2015).

5. Palies, P., Durox, D., Schuller, T., Candel, S. Nonlinear combustion instability analysis based on the flame describing function applied to turbulent premixed swirling flames. *Comb. and Flame,* **158**, 1980–1991, (2011).

6. Li, J. and Morgans, A.S. Time domain simulations of nonlinear thermoacoustic behaviour in a simple combustor using a wave-based approach *J. Sound Vib.,* **346**, 345–360, (2015).

7. Lipatnikov, A.N. and Chomiak, J. Turbulent flame speed and thickness: phenomenology, evaluation, and application in multi-dimensional simulations, *Progress in Energy and Combustion Science,* **28**, 1–74, (2002).

8. Iurashev, D., Campa, G., Anisimov, V., Di Vita, A., Cosatto, E., Daccà, F., and Albayrak, A. Turbulent Flame Models for Prediction of Pressure Oscillations in Gas Turbine Burners, *Proceedings of the 22nd International Congress on Sound and Vibration,* Florence, Italy, 12–16 July (2015).

9. Komarek, T. and Polifke, W. Impact of Swirl Fluctuations on the Flame Response of a Perfectly Premixed Swirl Burner, *J. Eng. Gas Turbines Power,* **132**, p. 061503-1,7, (2010) .

10. *OpenFOAM User Guide,* Version 2.3.0, 5 February (2014).

11. Polifke, W., Poncet, A., Paschereit, C. O., and Doebbeling, K. Reconstruction of acoustic transfer matrices by instationary computational fluid dynamics, *J. Sound Vib.,* **245**, (3), 483–510, (2001).

12. Poinsot, T.J. and Lele, S.K. Boundary Conditions for direct simulations of compressible viscous flows, *J. of Comp. Physics,* **101**, 104–129, (1992).

13. Tay-Wo-Chong, L. and Polifke, W. LES-Based Study of the Influence of Thermal Boundary Condition and Combustor Confinement on Premix Flame Transfer Functions, *ASME paper GT2012-68796*, (2012).